

LEGIBILITY NOTICE

A major purpose of the Technical Information Center is to provide the broadest dissemination possible of information contained in DOE's Research and Development Reports to business, industry, the academic community, and federal, state and local governments.

Although a small portion of this report is not reproducible, it is being made available to expedite the availability of information on the research discussed herein.

Received by mail

MAR 10 1989

Los Alamos National Laboratory is operated by the University of California for the United States Department of Energy under contract W-7405 ENG-36


TITLE VIBRATIONAL SPECTROSCOPIC INVESTIGATIONS OF SHOCK-COMPRESSED
LIQUID NITROGEN AND SHOCK-COMPRESSED LIQUID NITROMETHANE

AUTHOR(S) D. S. Moore and S. C. Schmidt

SUBMITTED TO Ninth Symposium (International) on Detonation

DISCLAIMER

This report was prepared as an account of work sponsored by an agency of the United States Government. Neither the United States Government nor any agency thereof, nor any of their employees, makes any warranty, express or implied, or assumes any legal liability or responsibility for the accuracy, completeness, or usefulness of any information, apparatus, product, or process disclosed, or represents that its use would not infringe privately owned rights. Reference herein to any specific commercial product, process, or service by trade name, trademark, manufacturer, or otherwise does not necessarily constitute or imply its endorsement, recommendation, or favoring by the United States Government or any agency thereof. The views and opinions of authors expressed herein do not necessarily state or reflect those of the United States Government or any agency thereof.

By acceptance of this article, the publisher izes that the U.S. Government retains a nonexclusive, royalty-free license to publish or reproduce the published form of this contribution, or to allow others to do so, for U.S. Government purposes.

The Los Alamos National Laboratory requests that the publisher identify this article as work performed under the auspices of the U.S. Department of Energy.

Los Alamos Los Alamos National Laboratory
Los Alamos, New Mexico 87545

VIBRATIONAL SPECTROSCOPIC INVESTIGATIONS OF SHOCK-COMPRESSED LIQUID NITROGEN AND SHOCK-COMPRESSED LIQUID NITROMETHANE *

D. S. Moore and S. C. Schmidt
Los Alamos National Laboratory
Los Alamos, New Mexico 87545

Vibrational spectra of liquid nitrogen and liquid nitromethane shock compressed to several high pressure/high temperature states were recorded using single-pulse multiplex coherent anti-Stokes Raman scattering. Vibrational frequencies were extracted from the data by computer spectral simulation techniques. Vibrational frequencies of liquid nitrogen were found to increase monotonically up to ≈ 17.5 GPa single shock and ≈ 30 GPa double shock and then to decrease with further increases in pressure. The consequence of the decrease in vibrational frequency on the Grüneisen mode gamma and its effect on the N_2 equation-of-state is discussed. A model is developed that includes the thermally-excited vibrational state transitions in the synthesized spectral fits of the nitromethane CARS data. The adequacy of the model for interpretation of CARS spectra in both ambient and shock-compressed nitromethane is discussed.

INTRODUCTION

Nitrogen is a relatively simple and stable diatomic molecule that has been studied over a wide range of pressure and temperature. Presently, there is renewed interest in this material, especially in the planetary sciences and in chemical explosives technology, because of the unusual effect high pressure and temperature have on its physical and chemical properties. Equation-of-state and thermodynamic data have been obtained for nitrogen at pressures up to 130 GPa and temperatures to beyond 10,000 K using both static¹⁻⁶ and dynamic⁷⁻¹¹ compression techniques. These measurements have been complemented by calculations for both the solid¹²⁻¹⁴ and fluid^{11,15-21} phases. The shock Hugoniot of liquid nitrogen exhibits an increase in compressibility above 30 GPa and 7000 K that has been attributed to a dissociative phase transition.^{10,16,18,22,23} Much recent experimental work has attempted to observe such a phase transition directly,^{24,25} or to provide further bulk property or molecular level evidence for such a phase transition.²⁶ The investigation reported on here²⁷ extends the pressure and temperature range of the measured fluid nitrogen vibrational frequency closer to the transition region in order to provide molecular level details about the behavior of this interesting material. Nitromethane is a prototypical homogeneous high explosive. As such, it has received considerable attention from a variety of researchers

Some recent progress has been made in the elucidation of the initiation mechanism,^{28,29} but much is still unknown. We also report here the results of an investigation into the behavior of the CN-stretching-mode vibrational frequency in shock-compressed liquid nitromethane.

EXPERIMENTAL METHODS

The high pressure/high temperature states investigated here were produced by dynamic compression techniques, and the vibrational spectra were recorded using coherent anti-Stokes Raman spectroscopy (CARS). The experimental apparatus has been described in detail previously.²⁷ Briefly, a projectile launched by a two-stage light-gas gun dynamically compressed a sample in a target designed to reflect the CARS signal back out an optical aperture. The cryogenic target assembly used to condense and hold liquid N_2 for these experiments has been described elsewhere,⁹ but was modified to include a highly polished 304 stainless steel target plate at the front and a 6.3 mm diameter quartz or lithium fluoride window at the rear. The room temperature targets used for nitromethane contained a similar sample chamber in a simple 150 mm diameter, 12 mm thick aluminum cylinder. Impactor and target plate thicknesses were chosen, and electrical time-of-arrival pin assemblies were installed in the liquid sample, so as to insure that rarefaction waves would not compromise the one dimensional character of the compression in the region observed optically.

*Work performed under the auspices of the U. S. Department of Energy

Pressures, densities, and temperatures for the singly- and doubly- shocked regions of N_2 were calculated using an effective spherical potential that has been shown to accurately reproduce both non-spherical molecular dynamics simulations and experimental Hugoniot and brightness temperature data.¹⁷⁻¹⁹ Doubly-shocked states were inferred from impedance matching of the N_2 shock, at the measured shock velocity, reflecting off the known window material assuming the theoretical equation of state for nitrogen. The equation-of-state parameters for the quartz and lithium fluoride windows are from published data.³⁰ The effect of the choice of potential was investigated by calculating pressures, densities and temperatures using Ross and Ree's corresponding states potential.¹⁶ These calculations resulted in very similar pressures and densities, but with an upward temperature shift of ~10%. The shock pressures in CH_3NO_2 were inferred using standard data reduction techniques³¹ and published shock-velocity/particle-velocity data.³⁰

CARS³² is a parametric process in which three waves, two at a pump frequency, ω_p , and one at a Stokes frequency, ω_s , are mixed in a sample to produce a coherent beam at the anti-Stokes frequency, $\omega_{as} = 2\omega_p - \omega_s$. The efficiency of this mixing is greatly enhanced if the frequency difference $\omega_p - \omega_s$ coincides with the frequency ω_j of a Raman active mode of the sample. The intensity of the beam at ω_{as} is given by

$$I_{as} \propto \sum_i \frac{\omega_{as}^2 \Gamma_j^{pk} N_i L_j^2 \left(\frac{n_{as}^2 + 2}{3} \right)^2 \left(\frac{n_s^2 + 2}{3} \right)^2 \left(\frac{n_p^2 + 2}{3} \right)^4}{n_p^2 n_{as} n_s} \times \left[\left(\sum_j \frac{\Gamma_j^{pk} (\omega_j - \omega_p + \omega_i)}{(\omega_j - \omega_p + \omega_i)^2 + \Gamma_j^2} + \chi^{nr} \right)^2 \cdot \left(\sum_j \frac{\Gamma_j^{pk} \chi_j^{pk}}{(\omega_j - \omega_p + \omega_i)^2 + \Gamma_j^2} \right)^2 \right] \quad (1)$$

where I_p and I_s are the incident intensities of the pump and Stokes beams, respectively and n_{as} , n_s , and n_p are the refractive indices at ω_{as} , ω_s , and ω_p , respectively. $N_i L_j$ corresponds to the Lagrangian density of the i th layer, and the sum is over noninterfering layers. χ^{nr} is the nonresonant susceptibility, χ_j^{pk} is the peak third-order susceptibility, and Γ_j is the half width at half maximum (HWHM) linewidth. The sum on j is over transitions. This equation only holds in the case of no electronic resonance enhancement.³²

The pump frequency in the CARS process was obtained by using approximately 40% of the 6 ns long frequency doubled output of a Nd:YAG laser (Quanta Ray DCR-1A) to pump a narrow band dye laser (Quanta Ray PDL-1) at near

557 nm for the nitrogen data, and near 605 nm for the nitromethane data. A broad range of Stokes frequencies was produced using a home-built broad-band dye laser utilizing the laser dye DCM (Exciton, lasing region 627 to 645 nm) pumped by the remaining Nd:YAG output. Some of the nitromethane data was obtained using the frequency-doubled Nd:YAG laser for the pump frequency and Rhodamine 590 (Exciton) in the broad-band dye laser for the Stokes frequencies. The CARS signals produced in the sample were directed through a 6 nm-band-width filter monochromator and then dispersed by a 1 m spectrometer. Multichannel detection of the CARS signals was done using an intensified photodiode array (Tracor Northern 6322) and analyzer (Tracor Northern 6500). In addition, the broad-band dye laser spectral profile was measured in each experiment using another 1 m spectrometer and an intensified photodiode array (Princeton Instruments IRY-512G) and analyzer (Princeton Instruments ST-100).

Phase matching was experimentally optimized in the ambient sample for the focusing conditions used. The dispersion in the sample was assumed to linearly scale with the increase in refractive index due to volume compression.³³ Linear scaling of the dispersion results in the same phase-matching angle at all compressions. The scaled refractive indices were also used in the local field correction terms of Equation (1).

Vibrational frequencies were all calibrated ($\pm 1 \text{ cm}^{-1}$) using vacuum wavenumbers of atomic emission lines obtained from standard calibration lamps. The spectral instrument function of the CARS spectrometer/photodiode array was measured using either an atomic emission line or by extraction from the ambient liquid nitrogen transition. The later method has the advantage of including the spectral profile of the pump laser. This measured instrument function was then convoluted with the synthesized CARS spectra to give spectra that could be directly compared with the experimental data.

RESULTS AND DISCUSSION FOR NITROGEN

We have obtained CARS spectra of fluid N_2 at many shock pressures and temperatures up to 21.3 GPa and 5020 K (single shock), and 40.8 GPa and 5160 K (reflected shock). Because of initial projectile velocity uncertainty and projectile tilt, the arrival time of the shock wave at the center of the target rear window (the location of the laser beam waists and the center of the rear time-of-arrival pin pattern) could only be predicted to 1.0 ns. For experiments where the shock wave had not reached the window, spectra corresponding to the solid curve in Fig. 1a were obtained. The large peak at 2328 cm^{-1} is the CARS signal from unshocked nitrogen and the remaining progression of lines are the

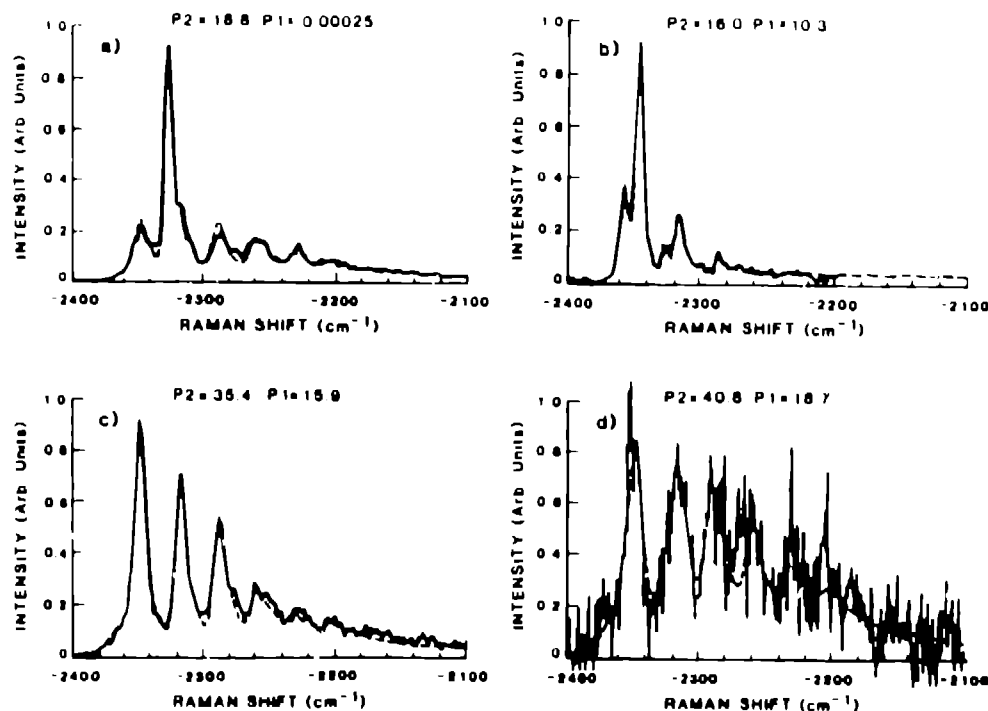


FIGURE 1. REPRESENTATIVE CARS SPECTRA OF SHOCK-COMPRESSED N_2

fundamental transition and hot bands from the singly-shocked fluid. Because unshocked liquid N_2 has a very narrow linewidth (0.029 cm^{-1} HWHM³⁴) compared to a width of several wavenumbers for the shock-compressed fluid, two difficulties were found. At the laser intensities used to produce CARS in the shock-compressed N_2 the CARS process either could be easily saturated³⁵ leading to an increase in the apparent linewidth of the ambient N_2 , or could result in large enough signals from the ambient N_2 to locally saturate the detector.

If the shock wave reached and reflected from the rear window, both the singly- and doubly-shocked regions in the sample were interrogated by the incident laser beams. The resultant spectra, similar to those depicted by solid curves in Figs. 1b, 1c, and 1d, consisted of two partially overlapped progressions of transitions arising from the two interrogated regions. Fig. 1b illustrates the case for which the lines have not broadened sufficiently to obscure the individual peaks of the two progressions. At higher shock pressures and temperatures, the lines broaden considerably (Fig. 1c) and it is difficult to distinguish the two progressions without a spectral simulation. Figure 1d is similar to the case of Fig. 1c, except with a much poorer signal-to-noise ratio. The results of the spectral simulations using Eq. (1) are shown in Fig. 1 by the dashed curves. The simulations assume that the linewidths of the fundamental and hot bands are the same

for a given shock pressure.

At the highest pressures investigated, the sample appeared to be a grey-body emitter. In the experiments near 21 GPa, photomultipliers monitoring the emission of the samples at 630 nm and at 520 nm recorded rise-times of the emission of several tens of ns. Significantly higher single-shock pressures resulted in much faster rise times. In addition, CARS signals became very difficult to observe at the higher pressures. The difficulty became especially acute after the shock had reached the window. By adjusting the timing to intentionally leave the shock short of the window when the CARS spectra were taken, data were successfully recorded near 21 GPa. Attempts to record CARS spectra above 22 GPa (single shock) have not yet been successful.

Figure 2 shows the Raman shifts extracted from the CARS spectra (using Equation (1)) of shock-compressed N_2 versus reduced density for the fundamental and observed hot band transitions. In the singly shocked material, there is a monotonic increase of the vibrational frequency with increasing density or pressure up to a compression of 2.23 (or a pressure of 17.5 GPa). Above this density the frequency no longer increases, and appears to begin to decrease. The vibrational frequency in the doubly-shocked material (whose temperature is lower than singly-shocked material of the same density) shows similar behavior, but the reversal

occurs at higher densities or pressures. It is interesting to note the effect of temperature in these data. When the fluid is singly or doubly shocked to the same density, the difference in measured Raman shift is due to the effects of temperature on the potential and on the portion of the potential sampled on average. Within the precision of the data, the anharmonicity of the intramolecular potential appears to be constant for all pressures and is the same as that expected from gas-phase data.

Static high pressure measurements of vibrational frequencies in solid nitrogen^{24,25} and solid hydrogen²⁵ show a similar reversal in the dependence of Raman shift with increasing pressure. Initial explanations of this effect invoked a change in the molecular electronic structure at the highest densities.²⁵ Recent isotopic mixture studies indicate that the reversal in the frequency shift in the molecular solids at high density is most likely due to resonant interactions (i.e. dynamic couplings between molecules).³⁶ Although in these experiments the sample remains a fluid, similar dynamic couplings may exist and may explain the reversal. Nevertheless, there still may be a temperature and density dependent alteration of the electronic structure in the fluid at the conditions encountered here. Alternatively, the ionization/dissociation mechanism proposed to explain the softening of the Hugoniot^{10,26} may be producing a sufficient density of charged species to affect the forces that influence the nitrogen vibrational frequency. Further progress towards identification of the operative mechanism might be gained using isotopic mixture studies.

Also plotted in Fig. 2 are the vibrational frequencies predicted by the pressure/temperature fit to the Monte Carlo simulation results.²¹ The published fit was adjusted, in the linear term only, so that the fit and the measured frequency agreed at our initial conditions. The simulation results show the correct trend with density up to $\rho/\rho_0 = 2.23$, where they level off with shock pressure rather than following the data as it appears to decrease. The simulations may be inadequate at these pressures and temperatures, however, for several reasons. For example, the nitrogen may be dissociating, which is not taken into account in the simulation. Additionally, ionization would introduce charges into the material that are not accounted for by the simulation.

The vibrational frequency data also allow the direct determination of single-mode Grüneisen parameters, $\gamma_i = -d \ln \omega_i / d \ln V$, for the vibrational modes. The γ_i for the fundamental transition was calculated from a smooth curve drawn through the measured Raman shifts and is presented in Fig. 3 for the single shock data. Note that this γ_i initially increases with decreasing volume (increasing pressure), then decreases rapidly and changes sign as the frequencies begin to decrease upon further decreases in

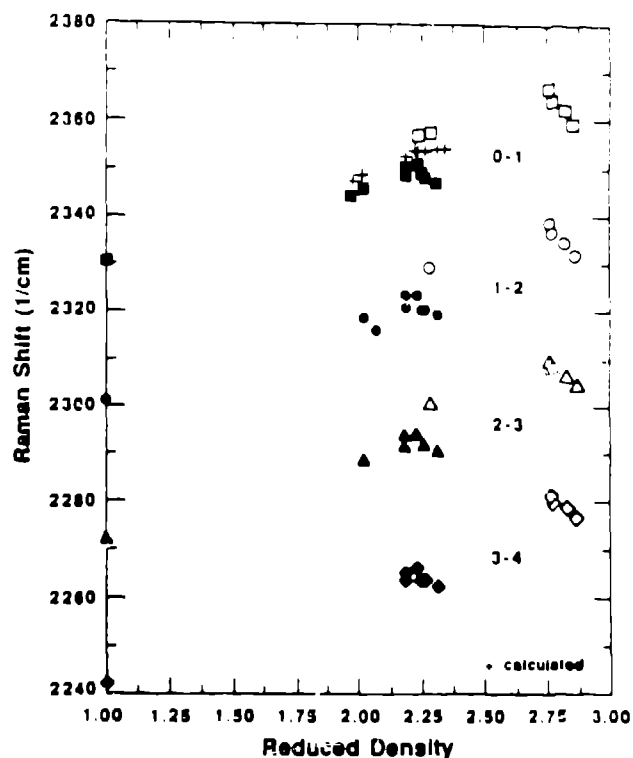


FIGURE 2. THE MEASURED N_2 RAMAN SHIFTS OF THE FUNDAMENTAL AND SEVERAL HOT BAND TRANSITIONS PLOTTED AGAINST REDUCED DENSITY. THE SOLID AND OPEN SYMBOLS REPRESENT SINGLE- AND DOUBLE-SHOCK DATA, RESPECTIVELY.

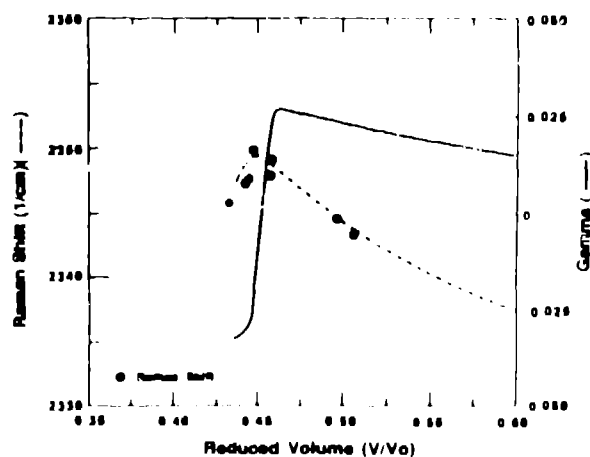


FIGURE 3. THE FUNDAMENTAL VIBRATIONAL MODE GRUENEISEN GAMMA (LINE) CALCULATED FROM THE SMOOTH CURVE (DASHED LINE) DRAWN THROUGH THE MEASURED RAMAN SHIFT PLOTTED VERSUS REDUCED VOLUME.

reduced volume below 0.47 (pressures above ≈ 15 GPa). The magnitude of the single mode γ_j , even at the maximum, is only a small fraction ($\approx 1\%$) of the total Gruneisen gamma for the fluid N_2 .²¹ Consequently, this interesting behavior of the vibrational mode gamma is not reflected in the N_2 equation of state. Although it may be said that this behavior of the vibrational modes has little consequence for the bulk behavior of this material, conversely it may be pointed out that this behavior provides further evidence that measurement of bulk properties provides very little information about molecular level details, which may be of larger importance in other materials, especially in chemically reactive systems.

RESULTS AND DISCUSSION FOR NITROMETHANE

For a polyatomic molecule such as nitromethane, the vibrational spectroscopy is considerably more complicated than that discussed above for the diatomic molecule N_2 . At low temperatures, only the vibrational fundamentals need be considered, leading to much simplification in the spectra. In the case of nitromethane, there are 15 possible vibrational normal modes, one of which is the nearly free rotation of the methyl group around the CN bond. If the molecule is assumed to possess C_{2v} symmetry when factoring the secular equation, the normal modes divide into 5 totally symmetric (A_1) modes, 5 modes parallel to the plane of the NO_2 (B_1), and 4 modes perpendicular to the NO_2 plane (B_2), with the torsion around CN being A_2 . Table I lists the literature frequencies of these vibrations obtained from Raman spectroscopy of the liquid.^{37,38} As temperature is increased, even just to room temperature, the low frequency modes start to become thermally populated to a measureable extent. The measured band contour is not just a collisionally-broadened

single vibrational frequency, but contains contributions from hot bands, not only from the thermal population of the level being probed, but also from the combination bands of the probed transition with all other thermally populated levels. This situation would still be completely tractable if all the anharmonicity constants, X_{jk} , were known. In the case of nitromethane, however, we could find only one reliable anharmonicity constant involving the vibration of interest in this work, namely the CN stretching mode, ν_4 .³⁷

In order to interpret the CARS spectra of shock-compressed nitromethane correctly, a model of the vibrational band contour was developed that includes the contributions of the hot bands. The relationship between CARS intensities and the spontaneous Raman cross section and vibrational-level populations can be approximated by:³²

$$\Gamma \chi_j^{pk} \frac{h}{2\pi c} \omega_p \omega_s = \left(\frac{d\sigma}{d\Omega} \right)_j (\rho_j - \rho_k) \quad (2)$$

where h is Planck's constant, c is the speed of light, $(d\sigma/d\Omega)_j$ is the spontaneous Raman cross-section of the j to k vibrational transition, and ρ_j and ρ_k are the number densities in vibrational levels j and k , respectively. For the CN-stretching mode transition in nitromethane discussed here, the j to k transitions all have $\Delta v_4 = 1$, and the ρ_j and ρ_k are all calculated assuming a Boltzmann population distribution among all the vibrational levels. A similar treatment was found to work well for shock-compressed liquid nitrogen.²⁷ The model then assumes that the ν_4 Raman cross section depends on ν_4 as prescribed for a harmonic oscillator, i.e. $(d\sigma/d\Omega)_{\nu_4} \propto (\nu_4 + 1)$. The cross section is further assumed to be independent of initial state v_j when $j \neq 4$.

The final step in the model is the determination of the frequencies of the possible hot bands that contribute to the contour of the CN stretching mode Raman spectrum. In the results presented here, the prescription of previous work is used,³⁹ wherein the anharmonic shift for a given vibrational band is proportional to the amount of vibrational energy in the lower state. That is,

$$\begin{aligned} X_{44} &= \frac{1}{2} A \nu_4, \\ X_{4j} &= A \nu_j \quad j \neq 4, \end{aligned} \quad (3)$$

where ν_j is the frequency of mode j . The parameter A is set from the measured position of the first overtone of ν_4 .⁴⁰ The anharmonicity coefficients calculated using equation (3) are listed in Table I. The frequency of a transition originating from the state $[v_j]$ is given by

TABLE I. FREQUENCIES, ASSIGNMENTS, DEGENERACIES AND CALCULATED ANHARMONIC COEFFICIENTS OF THE VIBRATIONAL MODES OF NITROMETHANE

ν_j (cm ⁻¹)	Assignment			g	X_{4k} (cm ⁻¹)
490	ν_6	b_1	$r(NO_2)$	1	-3.1
607	ν_8	b_2	$w(NO_2)$	1	-4.0
655	ν_5	a_1	$\delta(NO_2)$	1	-4.3
917	ν_4	a_1	$\nu(CN)$	1	.3
1096	ν_{11}	b_1, b_2	$r(CH_3)$	2	-7.2
1179	ν_3	a_1	$\delta_3(CH_3)$	1	-9.0
1402	ν_2	a_1	$\nu_3(NO_2)$	1	-9.2
1426	ν_{10}	b_1, b_2	$\delta_4(CH_3)$	2	-9.3
1561	ν_7	b_1	$\nu_4(NO_2)$	1	10.2

$$\nu(\nu) = \nu(0) + 2X_{11}\nu_1 + \sum_{k \neq 1} X_{1k}\nu_k \quad (4)$$

where $\nu(0)$ is the frequency of the $\Delta\nu_1 = 1$ transition originating from the vibrational ground state and is given by

$$\nu(0) = \omega_1 + X_{11} + \frac{1}{2} \sum_{k \neq 1} X_{1k} g_k$$

where ω_1 is the fundamental frequency of the ν_1 mode, and g_k is the degeneracy of mode k .

This model was used to calculate the positions and intensities of the hot bands of the CN stretching mode for ambient nitromethane and several shock-compressed pressure and temperature states of nitromethane. The first

observation of note is the improved fit of the synthetic CARS spectra to the ambient nitromethane CARS spectrum when using the above model, as is shown in figure 4. The low frequency side of the peak is not satisfactorily fit without inclusion of the available hot bands. For the CARS spectra of shock-compressed nitromethane, the vibrational levels change with pressure. Since not all the vibrational frequencies were measured in the shocked material, they were assumed to shift according to the available static high pressure results.⁴¹ However, since the measured frequency shifts in the shock-compressed liquid are slightly smaller than those measured in the static high pressure solid, the high pressure solid frequencies were all assumed to scale proportionally. The spectral fit of the shock-compressed nitromethane CARS spectrum in Fig. 5A is that given by the

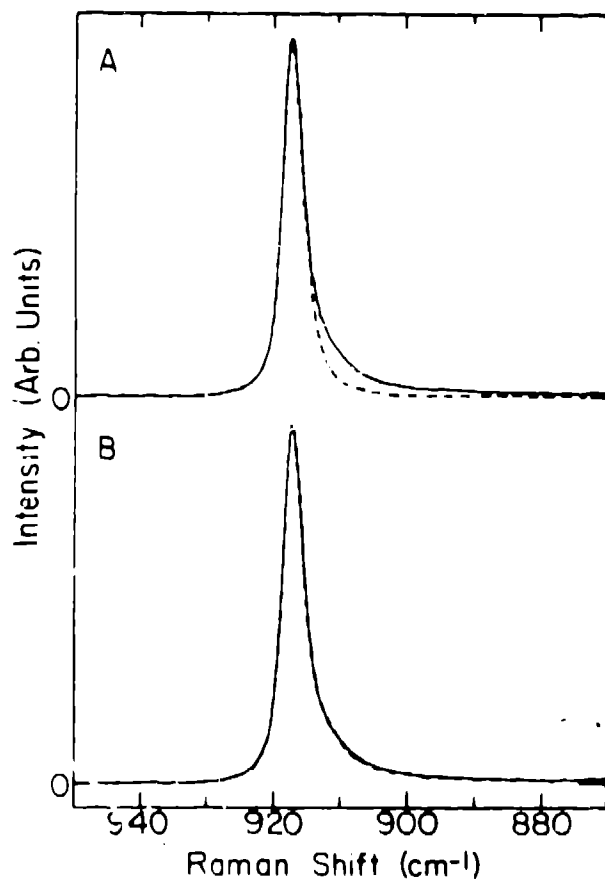


FIGURE 4. CARS SPECTRUM OF AMBIENT NITROMETHANE CN STRETCHING MODE. A) SYNTHETIC SPECTRUM (DASHED) INCLUDES NO HOT BANDS. B) SYNTHETIC SPECTRUM (DASHED) INCLUDES ALL POSSIBLE HOT BANDS.

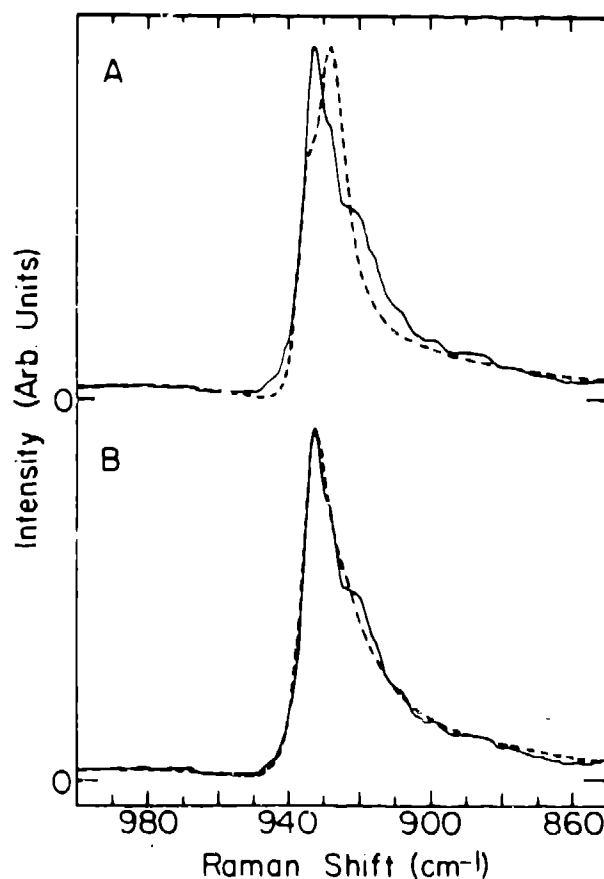


FIGURE 5. CARS SPECTRUM OF SHOCK-COMPRESSED LIQUID NITROMETHANE CN STRETCHING MODE. A) SYNTHETIC SPECTRUM (DASHED) WITH ALL HOT BANDS AND USING MODEL. B) SYNTHETIC SPECTRUM (DASHED) WITH ALL NON-DIAGONAL ANHARMONICITY COEFFICIENTS SET TO ZERO.

above model with the assumption that the anharmonic coefficients do not change with pressure. The linewidth of the transition was the only variable adjusted for the fit shown. The shock temperature was taken from the Lysne/Harderty equation of state.⁴² There is something obviously wrong with this model, which works well for the ambient liquid nitromethane CARS spectrum, when it is applied to the shock-compressed material, even at modest pressures and temperatures. The weakest approximation in the model is that of the values of the anharmonicity coefficients, and the assumption that they do not change with pressure. Since the n_4 vibrational frequency increases with pressure, indicated a stiffening of the potential for that motion, it might also become more resilient to the presence of other thermally populated vibrational motions. The consequence of this picture would be that the off-diagonal anharmonic coefficients would become small compared to X_{44} . Figure 5B shows a synthetic CARS spectrum assuming $X_{4j} = 0$, for $j \neq 4$, and only X_{44} and Γ are varied for the best fit. The quality of the fit in figure 5B is clearly better than that of 5A. The value of X_{44} used for 5B is only slightly larger than that used for the ambient spectrum. The increase may be indicative of some softening of the upper portion of the potential well with pressure. This behavior is somewhat different from that observed in nitrogen,²⁷ but may be due to the different depths of the wells or the different nature of diatomic molecules versus polyatomic molecules.

The apparent failure of the simple model presented here to satisfactorily represent the vibrational spectra of shock-compressed nitromethane suggests that intermolecular interactions can affect intramolecular potentials in sometimes surprising ways. Much further experimental work and substantial theoretical guidance will be necessary before these effects are fully understood.

ACKNOWLEDGEMENTS

We are indebted to John Chavez, John Chacon, Rick Eavenson, James Esparza, Concepcion Gomez, Vivian Gurele, Werner Haufchild, J. D. Johnson, Robert Livingston, David O'Dell, George Pittel, Dennis Price, Terry Rust, Dennis Shampine, and M. S. Shaw for their invaluable work in obtaining the results presented here. We appreciate the use of Joseph Fritz's MACRAME code that was used to calculate shock states, and Robert Caird's Fourier smoothing routines that were used in our data analysis. We are grateful to J. L. Lyman, R. S. McDowell and D. J. Taylor for enlightening discussions about polyatomic vibrational spectra. Finally, we are especially grateful to J. W. Shaner for his encouragement and support of this work.

REFERENCES

1. A. F. Schuch and R. L. Mills, J. Chem. Phys. Vol. 52, 6000 (1970).
2. R. L. Mills, D. T. Liebenberg, and J. C. Bronson, J. Chem. Phys. Vol. 63, 4026 (1975).
3. D. Schiferl, D. T. Cromer, and R. L. Mills, High Temp. High Pressures Vol. 10, 493 (1978).
4. D. Schiferl, S. Buchsbaum, and R. L. Mills, J. Phys. Chem. Vol. 89, 2324 (1985).
5. D. A. Young, C.-S. Zha, R. Boehler, J. Yen, M. Nicol, A. S. Zinn, D. Schiferl, S. Kinkead, R. C. Hanson, and D. A. Pinnick, Phys. Rev. E Vol. 35, 5353 (1987).
6. A. S. Zinn, D. Schiferl, and M. F. Nicol, J. Chem. Phys. Vol. 87, 1267 (1987).
7. V. N. Zubarev and G. S. Telegin, Soviet Physics - Doklady Vol. 7, 34 (1962).
8. R. D. Dick, J. Chem. Phys. Vol. 52, 6021 (1970).
9. W. J. Nellis and A. C. Mitchell, J. Chem. Phys. Vol. 73, 6137 (1980).
10. W. J. Nellis, N. C. Holmes, A. C. Mitchell, and M. van Thiel, Phys. Rev. Lett. Vol. 53, 1661 (1984).
11. G. L. Schott, M. S. Shaw, and J. D. Johnson, J. Chem. Phys. Vol. 82, 4264 (1985).
12. S. Nosé and M. L. Klein, Phys. Rev. Lett. Vol. 50, 1207 (1983).
13. R. LeSar, J. Chem. Phys. Vol. 81, 5104 (1984).
14. A. K. McMahan and R. LeSar, Phys. Rev. Lett. Vol. 54, 1929 (1985).
15. F. H. Ree and N. W. Winter, J. Chem. Phys. Vol. 73, 322 (1980).
16. M. Ross and F. H. Ree, J. Chem. Phys. Vol. 73, 6146 (1980).
17. M. S. Shaw, J. D. Johnson, and B. L. Hollan, Phys. Rev. Lett. Vol. 50, 1141 (1983).
18. J. D. Johnson, M. S. Shaw, and B. L. Hollan, J. Chem. Phys. Vol. 80, 1279 (1984).

19. M. S. Shaw, J. D. Johnson, and J. D. Ramshaw, J. Chem. Phys. Vol. 84, 3479 (1986).
20. R. LeSar and M. S. Shaw, J. Chem. Phys. Vol. 84, 5479 (1986).
21. J. Belak, R. D. Etters, and R. LeSar, J. Chem. Phys., to be published 1988.
22. M. Ross, in Shock Waves in Condensed Matter - 1987, edited by S. C. Schmidt and N. C. Holmes, North-Holland, Amsterdam, 1988, p. 95.
23. D. C. Hamilton and F. H. Ree, J. Chem. Phys., to be published 1989.
24. R. Reichlin, D. Schiferl, S. Martin, C. Vanderborgh, and R. L. Mills, Phys. Rev. Lett. Vol. 55, 1464 (1985).
25. P. M. Bell, H. K. Mao, and R. J. Hemley, Physica Vols. 139-140B, 16 (1986).
26. H. B. Radousky, W. J. Nellis, M. Ross, D. C. Hamilton, and A. C. Mitchell, Phys. Rev. Lett. Vol. 57, 2419 (1986).
27. D. S. Moore, S. C. Schmidt, M. S. Shaw, and J. D. Johnson, J. Chem. Phys., to be published 1989.
28. R. Engelke, Phys. Fluids Vol. 23, 875 (1980).
29. R. Engelke, D. Schiferl, C. B. Storm, and W. L. Earl, J. Amer. Chem. Soc., to be published 1988.
30. S. P. Marsh, LASL Shock Hugoniot Data, University of California Press, Berkeley, CA, 1980, p. 599.
31. M. H. Rice, R. G. McQueen and J. M. Walsh, Solid State Physics 6, Academic Press, New York, 1958, p. 1.
32. S. A. J. Druet and J. -P. E. Taran, Appl. Phys. Lett. Vol. 29, 174 (1976).
33. K. Vedam, in Critical Reviews in Solid State and Materials Sciences, edited by D. E. Schuele and R. W. Hoffman, CRC, Boca Raton, FL, 1983, p. 1.
34. S. A. Akhmanov, F. N. Gadjiev, N. I. Koroteev, R. Yu. Orlov, and I. L. Shumay, Appl. Opt. Vol. 19, 659 (1980).
35. I. L. Shumay, V. N. Zadkov, D. J. Heinzen, M. M. Kash, and M. S. Feld, Optics Lett. Vol. 11, 233 (1986).
36. Z. H. Yu, D. Strachan, and W. B. Daniels, Private Communication.
37. D. C. McKean and R. A. Watt, J. Mol. Spectrosc. Vol. 61, 184 (1976).
38. G. Malewski, M. Pfeiffer, and P. Reich, J. Mol. Structure Vol. 3, 419 (1969).
39. A. V. Nowak and J. L. Lyman, J. Quant. Spectrosc. Radiat. Transfer Vol. 15, 945 (1975).
40. R. Arndt and J. Yarwood, Chem. Phys. Lett. Vol. 45, 155 (1977).
41. D. Cromer, R. R. Ryan, and D. Schiferl, J. Phys. Chem. Vol. 89, 2315 (1985).
42. P. C. Lysne and D. R. Hardesty, J. Chem. Phys. Vol. 59, 6512 (1973).